**RESEARCH ARTICLE**

# Boosting endoplasmic reticulum folding capacity reduces unfolded protein response activation and intracellular accumulation of human kidney anion exchanger 1 in *Saccharomyces cerevisiae*

Xiaobing Li[1] | Emmanuelle Cordat[2] | Manfred J. Schmitt[1] | Björn Becker[1]

[1]Molecular and Cell Biology, Department of Biosciences and Centre of Human and Molecular Biology (ZHMB), Saarland University, Saarbrücken, Germany

[2]Department of Physiology and Membrane Protein Disease Research Group, University of Alberta, Edmonton, Alberta, Canada

**Correspondence**
Björn Becker and Manfred J. Schmitt, Molecular and Cell Biology, Department of Biosciences, Saarland University, Campus Building A 1.5, 66123 Saarbrücken, Germany.
Email: bjoern.becker@lih.lu; mjs@microbiol.uni-sb.de

## Abstract

Human kidney anion exchanger 1 (kAE1) facilitates simultaneous efflux of bicarbonate and absorption of chloride at the basolateral membrane of $\alpha$-intercalated cells. In these cells, kAE1 contributes to systemic acid–base balance along with the proton pump v-H$^+$-ATPase and the cytosolic carbonic anhydrase II. Recent electron microscopy analyses in yeast demonstrate that heterologous expression of several kAE1 variants causes a massive accumulation of the anion transporter in intracellular membrane structures. Here, we examined the origin of these kAE1 aggregations in more detail. Using various biochemical techniques and advanced light and electron microscopy, we showed that accumulation of kAE1 mainly occurs in endoplasmic reticulum (ER) membranes which eventually leads to strong unfolded protein response (UPR) activation and severe growth defect in kAE1 expressing yeast cells. Furthermore, our data indicate that UPR activation is dose dependent and uncoupled from the bicarbonate transport activity. By using truncated kAE1 variants, we identified the C-terminal region of kAE1 as crucial factor for the increased ER stress level. Finally, a redistribution of ER-localized kAE1 to the cell periphery was achieved by boosting the ER folding capacity. Our findings not only demonstrate a promising strategy for preventing intracellular kAE1 accumulation and improving kAE1 plasma membrane targeting but also highlight the versatility of yeast as model to investigate kAE1-related research questions including the analysis of structural features, protein degradation and trafficking. Furthermore, our approach might be a promising strategy for future analyses to further optimize the cell surface targeting of other disease-related PM proteins, not only in yeast but also in mammalian cells.

## Take Away

- We analysed the intracellular transport of human kAE1 to the yeast plasma membrane.

- We studied the effect of human kAE1 expression on yeast growth and UPR activation.
- We investigated the impact of different kAE1 truncation variants on UPR induction
- We implemented intervention strategies to improve PM targeting of kAE1.

## 1 | INTRODUCTION

*Saccharomyces cerevisiae* is often used to study specific aspects of various biological relevant cellular processes such as intracellular trafficking, signalling and/or protein degradation (Berner et al., 2018; Lashhab et al., 2019; Winters & Chiang, 2016). Aside from the high conservation of major cellular processes between yeast and humans, yeast cells further possess critical advantages compared with human cell culture including affordability and rapid cultivation, availability of a broad range of genetic manipulation tools (e.g., plasmid and knock-out strain collections) and the potential for performing high-throughput screening assays (Kolb et al., 2011; Mackie & Brodsky, 2018). Nevertheless, heterologous expression of human proteins often failed and/or ended up with proteins lacking their native function, localization and/or folding state (Bonar & Casey, 2010; Groves et al., 1999; Kolb et al., 2011; Romanos et al., 1992). A current example represents human kidney anion exchanger 1 (kAE1) which was found to be trapped in intracellular membrane structures after its heterologous expression in *S. cerevisiae* (Bonar & Casey, 2010; Groves et al., 1999; Sarder et al., 2020).

In humans, kAE1 is located at the basolateral membrane of α-intercalated cells (α-ICs) in the connecting tubules and the collecting duct and is part of a cellular machinery that regulates the acid–base homeostasis in the kidney (Lashhab et al., 2018; Roy et al., 2015). More precisely, membrane permeable $CO_2$ is normally enzymatically hydrated in α-ICs by carbonic anhydrase II (CA II) to carbonic acid ($H_2CO_3$). After spontaneous dissociation into $H^+$ and bicarbonate ($HCO_3^-$), kAE1 is responsible for the reabsorption of $HCO_3^-$ into the blood and the coupled influx of chloride ions ($Cl^-$) into α-ICs. At the same time, apically located v-$H^+$-ATPases mediate the excretion of $H^+$ into the urine. Consequently, proton excretion thus allows acid–base control in the kidney (Alper et al., 2002; Cordat & Casey, 2009; Lashhab et al., 2018). However, in mammals, mutations in kAE1 are associated with the development of a pathological phenotype, known as distal renal tubular acidosis (dRTA) (Alper, 2010; Lashhab et al., 2018; Trepiccione et al., 2017). Although it is speculated that some disease-causing kAE1 mutations lead to intracellular retention and/or mistrafficking of the anion transporter, the components of the intracellular kAE1 transport machinery are still not well characterized, and the actual role of the disturbed transport in dRTA is highly controversial (Cordat et al., 2006; Devonald et al., 2003; Lashhab et al., 2018; Toye et al., 2004).

Our recent study on human kAE1 indicated that yeast might represent a promising alternative model organism to address specific aspects of intracellular transport, function and degradation of complex membrane proteins (Sarder et al., 2020), although electron microscopy (EM) of kAE1-expressing yeast cells indicated that the majority of the protein accumulated in endoplasmic reticulum (ER)-derived membrane and/or vesicular structures, whereas only a minor fraction of biologically active kAE1 has reached the plasma membrane (PM) (Sarder et al., 2020). To fully benefit from the versatility of yeast in kAE1 studies, it would be desirable to optimize proper kAE1 targeting to the yeast PM by preventing and/or counteracting its intracellular accumulation. By performing colocalization studies with different organelle markers, we now visualize the intracellular trafficking of kAE1 from the ER to the PM and demonstrate its ability to enter the yeast secretory pathway. Our data indicate that kAE1 expression in yeast not only impairs cell growth but also induces a massive upregulation of the unfolded protein response (UPR). In a series of experiments using non-functional and truncated kAE1 variants, we further demonstrate that UPR activation and kAE1 accumulation partially depend on structural properties within the C-terminal region of kAE1. Our attempts to increase the ER folding capacity prevented the UPR response and, most importantly, strongly improved kAE1 trafficking to the cell periphery, resulting in an optimized model system for future studies on kAE1 transport in *S. cerevisiae*.

## 2 | RESULTS

### 2.1 | Precise kAE1 localization in the secretory pathway of *S. cerevisiae*

Recent EM data from yeast cells expressing different full-length kAE1 variants indicated that the majority of kAE1 accumulates in intracellular membrane and vesicle structures which most likely belong to the ER network. To enrich the pool of PM-localized kAE1 proteins, an *Δend3* deletion strain, defective in receptor-mediated and fluid-phase endocytosis, was used to eventually reduce the reinternalization of kAE1 from the yeast PM. Thereby, it was demonstrated that a

subpopulation of the anion transporter was capable to reach the yeast PM (Sarder et al., 2020). In Figure 1a, EM images of Δend3 cells expressing empty vector (EV) or HA-tagged kAE1 are illustrating the characteristic intracellular kAE1 accumulations. Nevertheless, the previous EM study was limited by an incomplete analysis of the exact intracellular kAE1 localization. Thus, it remained unclear if kAE1 accumulation only occurs in the ER or is also related to Golgi or endosomal structures.
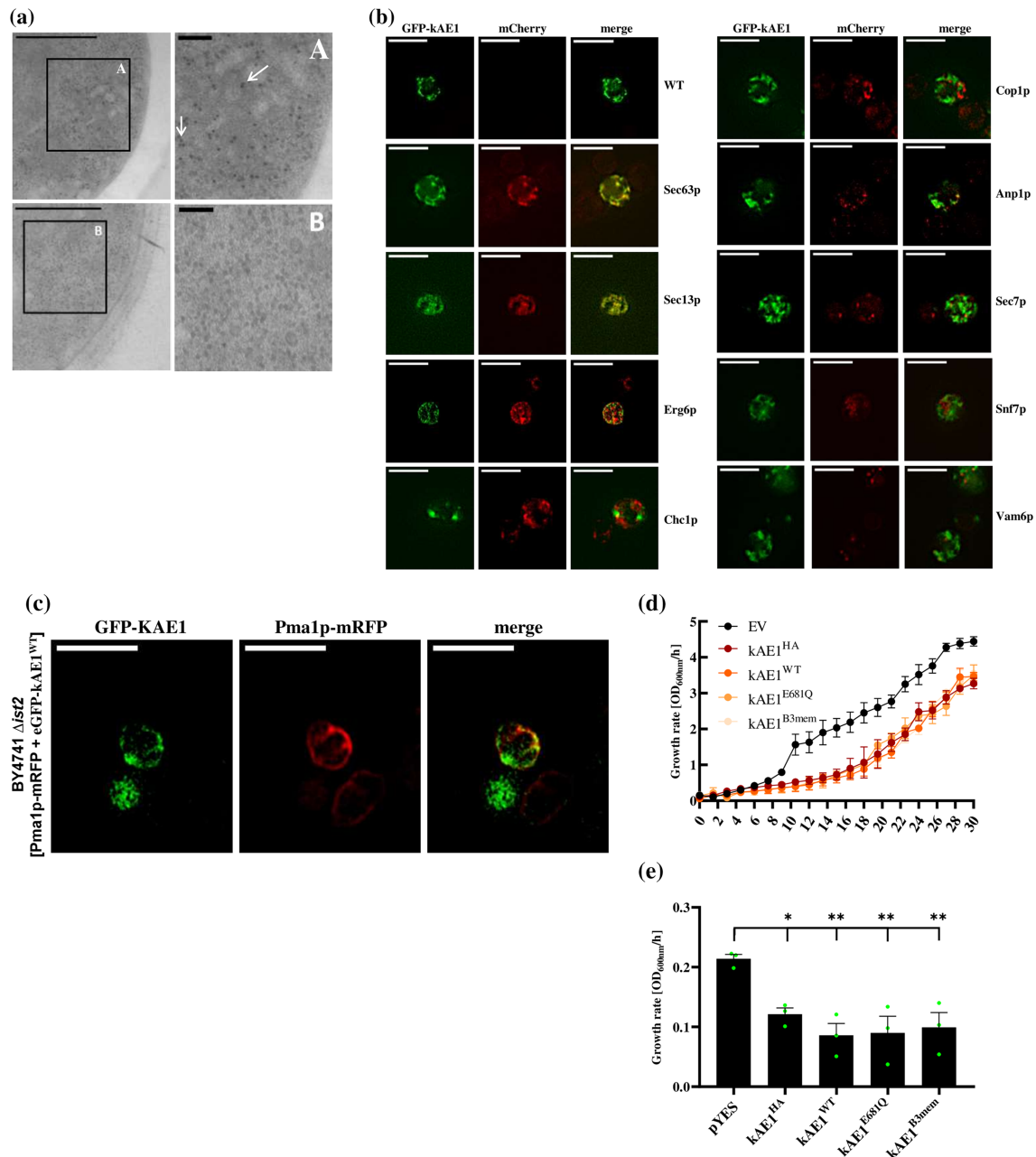


**FIGURE 1** kAE1 is predominantly localized in intracellular structures including endoplasmic reticulum (ER), cortical ER and COPII vesicles and reaches the yeast plasma membrane (PM). (a) (top) Electron microscopy (EM) images of typical membrane/vesicle (MV)-like structures (white arrows) induced by kAE1[HA] expression in Δend3 yeast cells. (bottom) Empty vector (EV) expression serves as negative control; scale bar: 500 nm. Inlets A and B show a magnified area of the marked regions (black box); scale bar: 100 nm. (b) Structured illumination microscopy (SIM) images of wild-type BY4742 cells expressing wild-type, eGFP-tagged kAE1 (GFP-KAE1) and different mCherry-tagged organelle marker proteins (mCherry: Sec63p = ER; Sec13p = COPII vesicles; Erg6p = cortical ER; Cop1p = COPI vesicle; Sec7p, Chc1p and Anp1p = Golgi; Snf7 and Vam6p = early and late endosome). kAE1 signals colocalized with Sec63p, Sec13p, Erg6p and Anp1p. Colocalization with other compartment markers was not visible; scale bar: 5 μm. (c) SIM images of BY4741 Δist2 cells expressing eGFP-kAE1[WT] (GFP-KAE1) and the chromosomal-integrated, mRFP-tagged PM marker Pma1p (mRFP); scale bar: 5 μm. (d) Growth curves and rates (OD$_{600}$/h) of wild-type BY4742 cells expressing the indicated kAE1 variants. Cells containing an EV pYES served as negative controls. Mean values ± SEM are indicated ($n = 3$) [Colour figure can be viewed at wileyonlinelibrary.com]

To precisely discriminate between the different secretory pathway subcompartments, localization of eGFP-tagged kAE1 (eGFP-kAE1) was verified in a first step via structured illumination microscopy (SIM) in various wild-type strains chromosomally expressing different mCherry-tagged organelle-specific marker proteins (Figures 1b and S1) (Weill, Arakel, et al., 2018; Weill, Yofe, et al., 2018). As previously suggested (Sarder et al., 2020), kAE1 showed colocalization with Sec63p (ER marker), Sec13p (COPII vesicle marker) and Erg6p (cortical ER marker) as evidenced by the yellow staining. Additionally, an overlap of kAE1 signals was visible with Anp1p (early Golgi marker). In contrast, kAE1 did not show any colocalization with other compartment markers (Sec7p, Vam6p, SNF7p, Cop1p and Chc1p). Although the majority of kAE1 signals showed an overlap with Sec63p (ER marker), the typical ring-like ER structure around the yeast nucleus was hardly detectable under kAE1 expression conditions (Figure 1b). Interestingly, GFP-kAE1 signal patterns showed striking similarities with the EM images of kAE1 expressing yeast cells, in which disturbed 'bubble'-like ER structures are flanked by intact ER regions (Sarder et al., 2020). Therefore, it is likely that kAE1 accumulation either disturbs or at least negatively affects the structure of the yeast ER.

Next, we further assessed whether N-terminal addition of eGFP affects kAE1 targeting to the yeast cell surface. It has already been described that N-terminal modifications do not affect kAE1 targeting to the cell surface in mammalian cells (Beckmann et al., 2002). By using fluorescence-based SIM, colocalization of kAE1 with the yeast PM was visible in Δ*ist2* cells expressing both eGFP-kAE1 and the PM marker Pma1p-mRFP (Figure 1c) (Grossmann et al., 2007; Papouskova et al., 2017), suggesting that the N-terminal eGFP fusion does obviously not prevent the PM targeting of kAE1 in yeast. However, we cannot completely exclude the possibility that an N-terminal modification of kAE1 impairs its proper in vivo transport. The additional deletion of *IST2*, a major tethering factor for PM/cortical ER contact sites, should thereby lead to a better separation of kAE1 signals located in cortical ER or PM structures (Manford et al., 2012; Sarder et al., 2020; Wolf et al., 2012).

In summary, our data demonstrate that full-length kAE1 is predominantly located in ER/cortical ER membrane structures, confirming the previous EM data and indicating that the anion transporter is not efficiently released from the yeast ER. However, colocalization of kAE1 with COPII vesicles, early Golgi compartment and PM demonstrates the potential delivery of a minor kAE1 pool through the secretory pathway to the yeast cell surface.

## 2.2 | Yeast cells expressing various kAE1 variants show cell growth defects

In yeast cells, it is known that heterologous expression of foreign proteins can cause cell growth defects often accompanied by ER stress induction (Kintaka et al., 2016). In order to verify whether kAE1 expression influences the growth behaviour of yeast cells, we determined growth rates of wild-type BY4742 cells expressing either various unmodified or HA/FLAG-tagged kAE1 or an EV. As illustrated in Figure 1d,e, cells expressing the EV showed the highest growth rate whereas the expression of the full-length kAE1 variants kAE1$^{WT}$ and kAE1$^{HA}$ significantly slowed cell growth. Interestingly, expression of N-terminally truncated kAE1 (kAE1$^{B3Mem}$) (Bonar & Casey, 2010; Groves et al., 1996) and an inactive kAE1$^{E681Q}$ variant (Jennings & Smith, 1992) lacking its bicarbonate exchange function did not improve cell growth.

## 2.3 | kAE1 expression induces UPR activation which is uncoupled from its bicarbonate exchange function

Both accumulation of kAE1 in ER membrane/vesicle structures and significantly slower cell growth rates are first indications for an overload of ER functions. To confirm our assumption, we monitored intracellular ER stress by measuring UPR activation with different biochemical approaches. Initially, Kar2p expression levels were verified via Western analysis (Figure 2a). In yeast, as a final step of the UPR signalling pathway, the transcription factor Hac1p upregulates a set of ER-luminal chaperones, such as Kar2p or Pdi1p, to increase the ER folding capacity (Sidrauski & Walter, 1997; Umebayashi et al., 1997). Consistent with the growth rate result, a massive Kar2p upregulation was not only detected in the presence of the UPR activators DTT and tunicamycin (TM), but it was also clearly visible after expression of the full-length kAE1 variants including kAE1$^{WT}$, kAE1$^{HA}$, kAE1$^{FLAG}$ and kAE1$^{E681Q}$. In contrast, DMSO treatment and overexpression of the HDEL receptor Erd2p, included in the analyses as marker for an endogenous yeast ER membrane protein, did not significantly alter Kar2p protein levels. To confirm the assumed kAE1 effect on UPR, Kar2p expression levels were calculated in cells showing a stepwise induction of kAE1$^{HA}$ expression using a genetically modified BY4742 wild-type strain containing a β-estradiol-inducible GEV promoter system (McIsaac et al., 2011). Indeed, a gradual and dose-dependent increase in Kar2p expression was detectable in kAE1$^{HA}$-expressing cells and not seen in negative control cells carrying an EV (Figure 2b,c), pointing towards an overload of the ER folding capacity.

Using strains containing a splicing reporter coupled to GFP or a *lacZ* reporter under transcriptional control of four UPR-responsive elements (Chang et al., 2004; Lajoie et al., 2012), we further support our initial findings. In addition, kAE1 expression always induced UPR activation, indirectly shown by increased cytosolic GFP expression via fluorescence microscopy and Western analysis (Figure S2A) or by β-galactosidase accumulation in cell lysates of kAE1-expressing yeast cells (Figure S2B).

To directly link kAE1 expression to UPR activation, Kar2p expression was finally validated in Δ*ire1* and Δ*hac1* cells expressing kAE1$^{HA}$. Under ER stress, Ire1p is able to detect misfolded proteins in the ER and activates translation of the transcription factor Hac1p by intron splicing of the inactive Hac1p pre-mRNA (Gardner & Walter, 2011; Sidrauski & Walter, 1997; Welihinda et al., 1999). Thus, deletion of either *IRE1* or *HAC1* should prevent UPR induction and Kar2p upregulation in the presence or absence of kAE1. As illustrated in
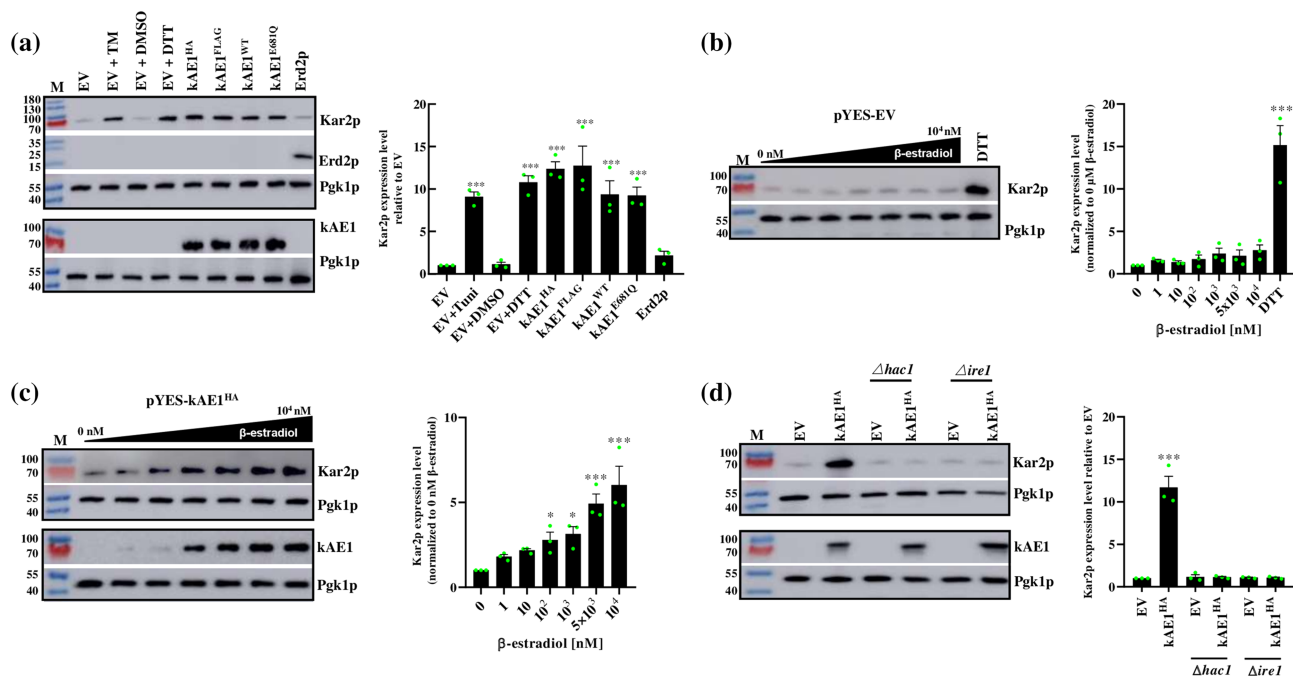
**FIGURE 2** kAE1 expression induces dose-dependent unfolded protein response (UPR) activation in yeast. (a) (left) Western blot analysis of BY4742 cells expressing empty vector (EV) pYES, HA or Flag-tagged kAE1 (kAE1^HA or kAE1^FLAG), unmodified wild-type (WT) kAE1 (kAE1^WT) or an inactive kAE1 variant (kAE1^E681Q). Cells expressing EV or V5-tagged Erd2p served as a yeast endogenous protein overexpression scenario. For UPR induction, cells containing EV were incubated 6 h with TM (dissolved in DMSO) or DTT. DMSO treatment served as negative control for TM samples. Western blot was probed with primary antibodies against Kar2p, kAE1 (anti-BRIC170), Erd2p (anti-V5) and the loading control Pgk1p and the corresponding HRP-coupled secondary antibodies. (right) Relative Kar2p expression level compared with the EV (normalized to Pgk1p). Mean values ± SEM ($n = 3$) are indicated ($^*p < 0.05$, $^{**}p < 0.01$ and $^{***}p < 0.001$, one-way ANOVA). (b,c) Western blot analysis of BY4742 GEV cells expressing the (b) EV pYES or (c) pYES-kAE1^HA in the presence of various β-estradiol concentrations (0, 1, 10, $10^2$, $10^3$, $5 \times 10^3$ and $10^4$ nM). Western blot was probed with primary antibodies against Kar2p, kAE1 (anti-BRIC170) and the loading control Pgk1p. Relative Kar2p expression level compared with EV (normalized to Pgk1p). Mean values ± SEM of three biological replicates ($n = 3$) are shown in the diagrams. (d) Western blot analysis of WT, Δhac1 and Δire1 BY4742 cells expressing EV pYES or kAE1^HA. Western blot was probed with primary antibodies against Kar2p, kAE1 (anti-BRIC170) and the loading control Pgk1p. Mean values ± SEM ($n = 3$) are indicated ($^*p < 0.05$, $^{**}p < 0.01$ and $^{***}p < 0.001$, one-way ANOVA) [Colour figure can be viewed at wileyonlinelibrary.com]

Figure 2d, Δire1 and Δhac1 cells expressing kAE1^HA did not show any upregulation of Kar2p, indicating that kAE1 expression directly activates the Ire1p-mediated UPR signalling pathway in yeast.

Taken together, all these findings indicate that yeast cells expressing kAE1 variants show Ire1p-dependent UPR pathway activation. Neither the removal of the N-terminal cytosolic region (kAE1^B3Mem) nor the elimination of the bicarbonate exchange function (kAE1^E681Q) was capable of preventing the UPR induction in *S. cerevisiae*.

## 2.4 | Structural kAE1 yeast homologue Bor1p shows striking similarities in UPR induction

So far, it seems that the intensity of UPR activation correlates with the level of kAE1 expression, similarly to numerous other protein overexpression studies that have previously described this accumulation phenomenon (Sarder et al., 2020; Umebayashi et al., 1997). It is plausible that an overload of the cellular folding machinery in the ER inevitably results in an accumulation of misfolded proteins such as kAE1 in this study. However, the effect of kAE1 was out of scale

compared with the overexpression of the yeast HDEL receptor Erd2p. For this reason, we asked to which extent the expression of other yeast membrane proteins, including the structural yeast kAE1 homologue Bor1p (Coudray et al., 2017; Thurtle-Schmidt & Stroud, 2016), influence UPR induction by determining Kar2p protein levels (Figure 3a). As expected, expression of all yeast membrane proteins— with exception of the yeast HDEL receptor Erd2p—led to a significant UPR activation indirectly seen by increased Kar2p expression levels. Surprisingly, Bor1p showed the strongest UPR induction of all yeast proteins. Taking into account that kAE1 expression level was two times higher than Bor1p, both proteins show a similar, disproportional effect on ER stress induction. Therefore, the mere expression did not seem to be the sole determinant for the massive UPR activation.

## 2.5 | Structural features in the C-terminal region of kAE1 contribute to UPR induction in yeast

Given the structural homology between Bor1p and kAE1, we further asked if structural features might play a role in Ire1p-mediated UPR
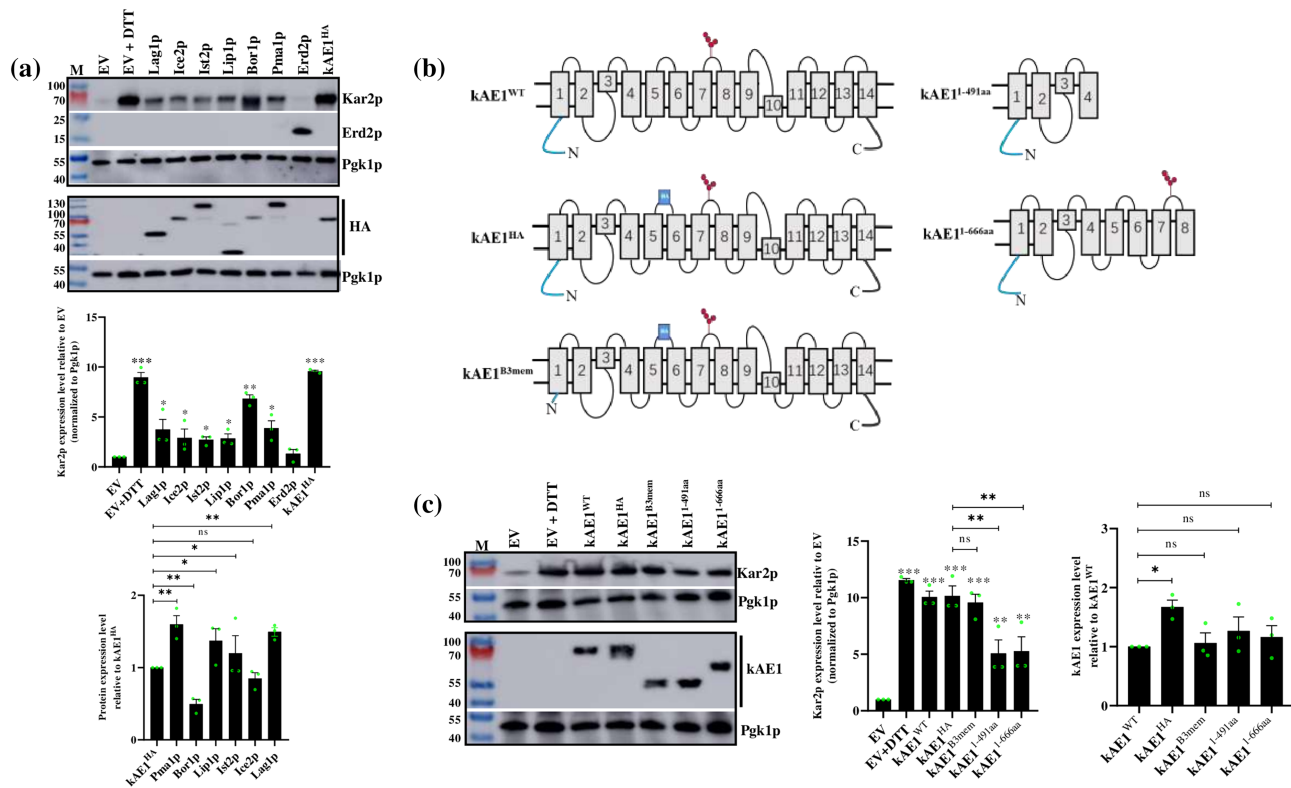
**FIGURE 3** Structural properties of the kAE1 C-terminus are involved in unfolded protein response (UPR) activation in yeast. (a) Effect of membrane protein overexpression on UPR activation in yeast. (top) Western blot analysis of wild-type BY4742 cells expressing various HA-tagged yeast membrane proteins or kAE1[HA]. As negative control, cells contain only an empty vector (EV) pYES. To activate UPR, cells were pretreated with DTT for 6 h (EV + DTT). Western blot was probed with primary antibodies against Kar2p, Erd2p (anti-V5) and the loading control Pgk1p. Anti-HA antibodies were used to detect expression of kAE1[HA] and the different yeast membrane proteins. (middle) Relative Kar2p expression level compared with EV situation (normalized to Pgk1p). Mean values ± SEM ($n = 3$) are indicated (*$p < 0.05$, **$p < 0.01$ and ***$p < 0.001$, one-way ANOVA). (down) Relative kAE1 expression level in the different overexpressing strains (relative to kAE1[HA]). Mean values ± SEM ($n = 3$) are indicated (*$p < 0.05$, **$p < 0.01$ and ***$p < 0.001$, one-way ANOVA). (b) Schematic outline of various wild-type and truncated kAE1 variants used in (c). The cytosolic N-terminus kAE1 is shown in blue and the cytosolic C-terminus in black. Additionally, the $N$-glycosylation site (Asn[577]) and the HA-epitope tag (HA) are illustrated in the different constructs. (c) (left) Western analysis of BY4742 cells expressing EV pYES, kAE1[HA], kAE1[WT] and C-terminal and N-terminal truncated kAE1 variants (kAE1[B3mem], kAE1[1-491aa] and kAE1[1-666aa]). EV cells in the absence (EV) or presence of DTT (EV + DTT) serve as negative and positive control for UPR induction. Blot was probed with primary antibodies against Kar2p, kAE1 (anti-BRIC170) and the loading control Pgk1p. (middle) Relative Kar2p expression level compared with EV situation (normalized to Pgk1p). Mean values ± SEM ($n = 3$) are indicated (*$p < 0.05$, **$p < 0.01$ and ***$p < 0.001$, one-way ANOVA). (right) kAE1 expression level relative to kAE1[WT] [Colour figure can be viewed at wileyonlinelibrary.com]

activation. Therefore, C-terminal and N-terminal truncated variants of the anion exchanger were generated (Figure 3b), and their impact on UPR activation was monitored via Kar2p expression levels (Figure 3c). kAE1[1-666] is lacking the cytosolic C-terminus and transmembrane domains (TMD) 10 to 14, whereas kAE1[1-491] is missing the $N$-glycosylation site at position Asn[577] (according to Asn[642] in AE1) and TMD 5 to 14 (Reithmeier et al., 2016). Because $N$-glycosylation of full-length kAE1 was not detected in *S. cerevisiae* (Bonar & Casey, 2010; Sarder et al., 2020) and it is reported that deglycosylation probably affects the folding and aggregation state of kAE1 in oocytes, we asked whether Asn[577] plays a specific role in UPR induction (Groves & Tanner, 1994). Based on the AE1 crystal structure (Reithmeier et al., 2016), both variants should be unable to retain an intact core and/or gate domain; however, our data of kAE1[E681Q] already suggest that kAE1 function is not responsible for

the observed UPR induction. As shown in Figure 3c, cells expressing kAE1[1-491] and kAE1[1-666] displayed a significantly reduced Kar2p expression level compared with both kAE1[WT]- and kAE1[HA]-expressing cells. Additional truncation of the cytosolic N-terminus in kAE1[B3Mem] did not reduce Kar2p protein levels, excluding a specific role of the cytosolic N-terminus in UPR activation. Because the expression level of all truncated versions did not dramatically differ from unmodified kAE1[WT] (Figure 3c), variation in protein expression levels could be excluded as origin of the reduced UPR activation seen in kAE1[1-491] and kAE1[1-666]. Interestingly, both variants did not completely prevent Kar2p upregulation (reduction of around 50% compared with kAE1[WT]) but showed very similar reduction levels, indicating that the lack of TMD 10–14 and/or the cytosolic C-terminus in kAE1[1-666] are crucial for UPR induction in yeast. In contrast, removal of TMD 5–9 and Asn[577] did not further decrease Kar2p

expression levels and, therefore, might not be important for UPR induction (Figure 3c).

## 2.6 | Increased ER folding capacity reduces UPR activation in kAE1 expressing cells and significantly improves kAE1 transport to the cell periphery

Finally, we searched for solutions to counteract the accumulation and UPR activation induced by full-length kAE1 expression. In yeast, different strategies have already been reported to enhance the folding and secretion capacity of the ER and, thereby, improving proper protein folding and/or targeting in the secretory pathway. Here, we tested whether the additional overexpression of different ER proteins involved in protein folding influences UPR activation. As shown in Figure 4a, under strong galactose-induced kAE1 expression conditions, we could not observe any effect on Kar2p expression after

over expression. However, if kAE1 expression was decreased by using a β-estradiol-inducible expression system which allows a dose-dependent kAE1 expression regulation, a significant reduction of Kar2p expression was observed in cells expressing Pdi1p or Emc1p. In contrast, the effect was not visible in EV control cells (Figure 4b). Because relative kAE1 expression levels did not significantly differ between all strains, the missing upregulation of Kar2p is presumably mediated by the increased ER folding capacity after additional ER chaperone expression (Figure 4b). These findings nicely indicate that an improved kAE1 folding can prevent kAE1-mediated UPR induction in yeast. Consistently, if one would expect that more correctly folded kAE1 is present under these conditions, an improved kAE1 processing within the secretory pathway and trafficking to the yeast PM should take place. Indeed, a drastic shift in the localization of kAE1 was visible in SIM images. As expected and illustrated in Figure 4c, cells simultaneously expressing eGFP-kAE1 and the EV pBG1805 showed a distinct overlap of kAE1 signals (green) with the mCherry-labelled
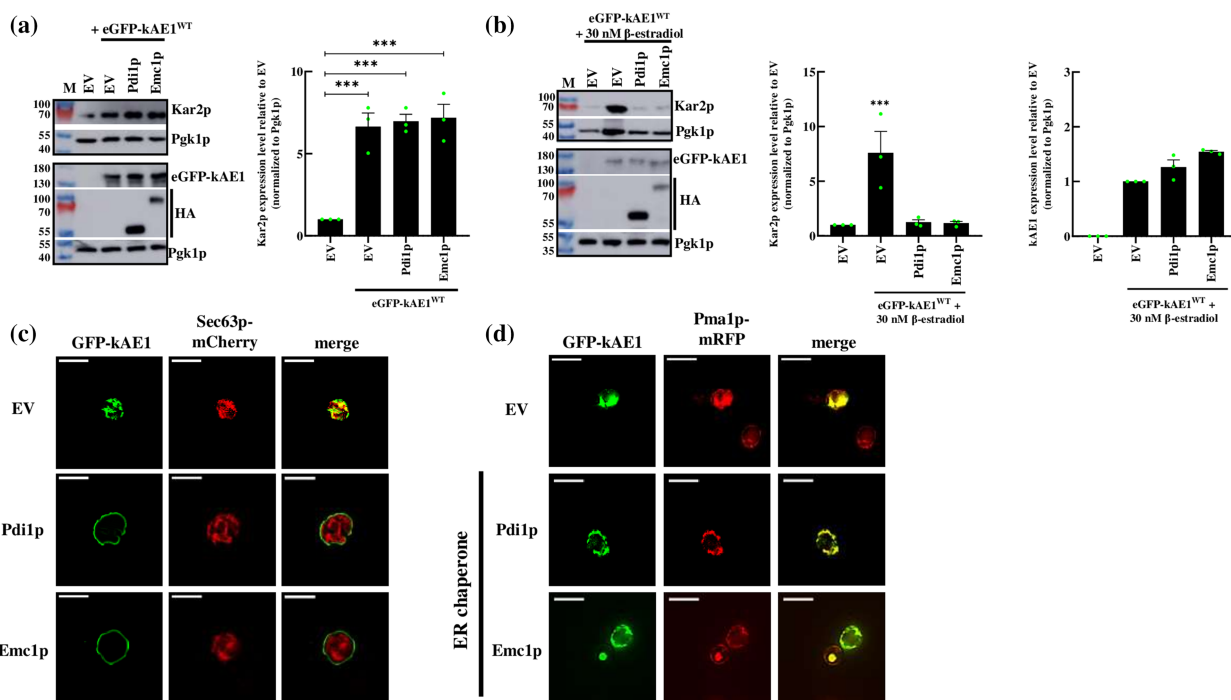


**FIGURE 4** Increased endoplasmic reticulum (ER) folding capacity reduces unfolded protein response (UPR) activation. (a) (Top) Western analysis of BY4742 cells expressing eGFP-kAE1$^{WT}$ together with the empty vector (EV) pBG1805 or the indicated yeast ER chaperones. EV cells without an additional kAE1 plasmid served as negative control. Blot was probed with primary antibodies against Kar2p, kAE1 (anti-BRIC170) and the loading control Pgk1p. Anti-HA antibodies were used to detect expression of the different ER chaperones. (Down) Relative Kar2p expression level compared with EV situation (normalized to loading control pPgk1p). Mean values ± SEM ($n = 3$) are illustrated. (b) (left) Western analysis of BY4742 GEV cells expressing eGFP-kAE1$^{WT}$ together with the EV pBG1805 or the indicated yeast ER chaperones. kAE1 expression was induced with 30-nM β-estradiol. EV cells without an additional kAE1 plasmid served as negative control. Blot was probed with primary antibodies against Kar2p, kAE1 (anti-BRIC170) and the loading control Pgk1p. Anti-HA antibodies were used to detect expression of the different ER chaperones. (middle) Relative Kar2p expression level compared with EV situation (normalized to loading control pPgk1p). (right) Relative kAE1 expression level compared with EV situation (normalized to loading control Pgk1p). Mean value ± SEM ($n = 3$) are illustrated (*$p < 0.05$, **$p < 0.01$ and ***$p < 0.001$, one-way ANOVA). (c) Structured illumination microscopy (SIM) images of yeast cells expressing mCherry-tagged ER marker Sec63p (mCherry) together with the eGFP-tagged kAE1 (GFP-KAE1) and the indicated ER chaperones. pBG1805 (EV) served as negative control without any ER chaperone expression. Scale bar: 5 μM. (d) SIM images of yeast cells expressing mRFP-tagged PM marker Pma1p (mRFP) together with the eGFP-tagged kAE1 (GFP-KAE1) and the indicated ER chaperones. EV pBG1805 served as negative control. Scale bar: 5 μM [Colour figure can be viewed at wileyonlinelibrary.com]

ER marker Sec63p (red). In contrast, additional expression of ER chaperones led to a dramatic change in the intracellular kAE1 localization. All cells showed a similar GFP signal distribution in the form of ring-like structures at the cell periphery. Moreover, SIM experiments with an mRFP-labelled PM marker (Pma1p) showed colocalization of the peripheral GFP signals with the yeast PM (Figure 4d). These data strongly support our hypothesis that misfolded kAE1 accumulates in the ER, whereas an improved ER folding capacity is capable to at least partially restore the native folding state of the anion transporter under a regulated and dose-dependent kAE1 expression system.

## 3 | DISCUSSION

Various studies in the last decades have highlighted the model organism yeast as alternative expression platform for human proteins to investigate fundamental cellular processes including protein degradation, biosynthesis and transport (Sarder et al., 2020). However, heterologous expression of human proteins (e.g., membrane proteins) is not trivial and lack of expression and/or loss of function are common issues in this context (Bonar & Casey, 2010; Groves et al., 1999; Kolb et al., 2011). Furthermore, the use of strong promoters and multicopy vectors exceed in many cases the folding capacity of yeast cells, causing aggregation and/or accumulation of misfolded proteins (Kintaka et al., 2016; Umebayashi et al., 1997). Most recently, we have performed a pilot study in *S. cerevisiae* showing the successful expression of full-length variants of the human kAE1 with correct PM localization and biological activity. Nevertheless, a major drawback of the current model system was the tremendous kAE1 accumulation observed in intracellular compartments and low abundance of PM-localized kAE1 (Sarder et al., 2020).

By performing colocalization experiments with fluorescently labelled kAE1 and organelle markers for the secretory pathway, we now provide a more precise picture of the intracellular kAE1 trafficking in yeast. As expected from our previous EM analyses (Sarder et al., 2020), the vast majority of full-length kAE1 colocalizes with ER and cortical ER structures. However, some kAE1 signals overlap with the COPII vesicle marker Sec13p and the Golgi marker Anp1p, indicating an anterograde transport of kAE1 from the ER to the Golgi apparatus. Additionally, early and late endosomal compartment markers did not show any colocalization with the fluorescent anion transporter whereas the overlap of kAE1 with the PM marker Pma1p was clearly visible. Because the colocalization experiments of kAE1 and Pma1p were performed in the genetic background of a yeast Δist2 mutant, it is most likely that the overlap is not caused by kAE1 signals derived from the cortical ER. Surprisingly, our data showed costaining with Golgi structures and PM but not with endosomal structures. In our opinion, the most likely explanation for this observation is an endosome-independent transport of kAE1 directly from the trans-Golgi network (TGN) to the yeast PM. In yeast, several alternative PM transport routes (e.g., exomer) have been described which allow direct cargo transport from the Golgi to the cell surface (Spang, 2015; Wang et al., 2006). Furthermore, endosome-independent

trafficking pathways are also found in mammalian cells (Chen et al., 1998; Parmar & Duncan, 2016; Wakana et al., 2012). Interestingly, it has been postulated that kAE1 can reach the PM by an endosome-independent transport mechanism (Junking et al., 2014). Alternatively, the lack of colocalization with endosomal markers may simply reflect the transitory nature of the colocalization in endosomes that was not captured in our pictures. In the future, it would be interesting to study the exit of kAE1 from the yeast TGN in more detail to address how adequate the yeast model system can mimic the native PM targeting of kAE1 in mammalian cells.

Based on our biochemical data, it is obvious that heterologous kAE1 expression induces a massive UPR response in *S. cerevisiae*. Both upregulation of the ER chaperone Kar2p and the increased activation of UPR-responsive elements demonstrate that yeast cells show an increased stress response in the presence of kAE1. Consistently, inactivation of the Ire1p pathway by using Δire1 and Δhac1 cells completely prevented Kar2p induction under induced kAE1 expression. Because UPR activation represents a cellular response to misfolded proteins (Kimata & Kohno, 2011), we conclude that the majority of newly synthesized kAE1 is not properly folded and, hence, predominantly aggregates and/or accumulates in the yeast ER. Consequently, the release of misfolded kAE1 from the ER is interrupted, resulting in its inefficient targeting to the cell surface. Diminished growth rates under kAE1 expression further support our hypothesis. Interestingly, neither inactive kAE1[E681Q] nor N-terminally truncated kAE1[B3Mem] was capable of restoring cell growth and of preventing UPR response.

Previous yeast studies already speculated that structural features in the N-terminal region of kAE1 might be the reason for its intracellular ER retention (Groves et al., 1999). Because removal of the N-terminus did not show an increased PM localization in the previous EM study (Sarder et al., 2020) and did not show an impact on UPR induction, it is unlikely that this region plays an essential role in intracellular kAE1 retention. However, we now demonstrate that structural features in the C-terminus encompassing TMD 9–14 and the cytosolic carboxyl-terminus are partially involved in the ER stress induction of kAE1 expressing cells (Figure 3b,c). Surprisingly, the structural kAE1 homologue Bor1p showed a comparably high UPR response after its overexpression whereas the expression of other yeast membrane proteins only moderately induced the upregulation of the ER stress indicator Kar2p (Coudray et al., 2017; Thurtle-Schmidt & Stroud, 2016). Remarkably, overexpression of the yeast HDEL receptor Erd2p that served as a yeast endogenous protein overexpression scenario did not significantly activate the UPR pathway in yeast cells. Due to HDEL-dependent retention function, the increased cellular Erd2p quantity presumably accelerates the retrieval of ER-luminal proteins back to the ER. Because most ER chaperones, including Kar2p and Pdi1p, contain C-terminal HDEL-retention motifs, a higher ER folding capacity could be expected which simultaneously prohibits the accumulation of misfolded and UPR-inducing proteins (Becker et al., 2016; Semenza et al., 1990).

Our hypothesis that structural features in kAE1 and Bor1p trigger Ire1p-mediated UPR induction was supported by additional truncation

experiments. Indeed, the expression of shorter kAE1 variants lacking parts of the C-terminal region (kAE1$^{1-491aa}$ and kAE1$^{1-666aa}$) significantly reduced cellular Kar2p levels. Given that Kar2p upregulation is dose dependent and not completely abolished in the truncated variants, we therefore speculate that structural properties between TMD 10–14 and the cytosolic C-terminus are required for the kAE1-induced UPR activation in yeast. However, a more detailed analysis of other truncated kAE1 variants is required to precisely map the C-terminal region responsible for the reduced UPR activation. It is likely that the cytosolic C-terminal part of kAE1 induces the UPR phenotype. In mammalian cells, it is known that the cytosolic C-terminus represents an interaction hotspot that modulates the proper transport of kAE1 to the basolateral membrane (Almomani et al., 2012; Su et al., 2011; Su et al., 2017; Toye et al., 2004). Theoretically, the mere lack of such an interaction partner required for proper folding could induce the observed accumulation and misfolding of kAE1 in yeast. In this context, simultaneous coexpression of glycophorin A, a known kAE1 interaction partner, was shown to improve the PM targeting of kAE1 in yeast cells and frog oocytes (Groves et al., 1999; Groves & Tanner, 1992; Young et al., 2000). However, it should be noticed that several known dRTA-causing mutations are located in this C-terminal kAE1 region from TMD 10 to 14 (p.R901X, p.D905dup, p.D905Gfs15, p.E906K and p.M909T). A couple of these mutations (e.g., p.G701D or p.S773P) also lead to incorrect folding and/or distinct trafficking defects such as ER or Golgi retention in mammalian MDCK cells (Cordat et al., 2006). In future studies, it would be interesting to understand to which extend these mutations trigger UPR activation in mammalian cells and if chemical chaperones or coexpression of ER chaperones can prevent kAE1 mistrafficking and eventually restore kAE1 functionality in α-ICs.

To perform a genome-wide screening for potential kAE1 transport modulators, the inefficient kAE1 targeting to the secretory pathway represents a major drawback of the model system introduced by Sarder et al. (2020). However, our present data provide a first strategy to overcome this issue and optimize the yeast model system for future transport screening studies. Surprisingly and unexpected, overexpression of an individual ER chaperone not only prevents UPR activation under moderate kAE1 expression levels but also dramatically improves PM targeting of kAE1. These results further strengthen the idea that kAE1 misfolding in the ER is the major bottleneck for studying kAE1 trafficking in yeast. However, UPR activation was not prevented if kAE1 expression exceeds a certain limit, demonstrating that a fine-tuning of the expression parameters is crucial to achieve optimized conditions for kAE1 folding and trafficking. Notably, the selection of the yeast strain has also a strong impact on the kAE1 distribution at the yeast PM. Although BY4741 and BY4742 cells show a clear kAE1 localization at the PM after ER chaperone overexpression, the fluorescence pattern in BY4741 and BY4742 cells differs. Although the microscopic and biochemical results strongly support our hypothesis that kAE1 is more efficiently folded and transported to the PM after expanding the ER folding capacity, future EM studies in analogy to the previous EM study would be essential to finally prove our assumption (Sarder et al., 2020).

It should be noticed that overexpression of cytosolic and ER-localized chaperones is a widely used strategy to prevent or counteract the misfolding and aggregation of various proteins in different species. For example, the commercially available GroEL-GroES system from *Escherichia coli* is often used in bacteria to improve the yield and biological activity of recombinantly expressed proteins (Lamppa et al., 2013; Nishihara et al., 1998). Previous studies already used Kar2p (BiP) or Pdi1p overexpression in *S. cerevisiae* to boost the secretion of recombinant proteins including β-glucosidase, α-amylase and others (Hou et al., 2012). It is further reported that the expression of Hsp70, Hsp90 and BiP can prevent and/or rescue the misfolding of disease-related PM proteins. Therefore, Pdi1p represents a potential candidate not only to improve PM transport of kAE1 but also to foster PM targeting of other kidney disease-related proteins which have already been studied in yeast as model organism (e.g., aquaporins and CTFR) (Kolb et al., 2011). So far, Emc1p overexpression has not been described as a strategy to improve PM targeting of membrane proteins in yeast cells. Because Emc1p forms a heteromeric complex with five other proteins (Emc2–Emc6) (Shurtleff et al., 2018), it could be interesting in the future to understand how Emc1p affects the expression status of the other complex members and to clarify whether or not the expression of other Emc proteins has a comparable effect on kAE1 redistribution to the cell surface.

Based on our current findings, kAE1-related research questions should be ideally addressed in a BY4741 strain background expressing a yeast codon-optimized full-length kAE1 under the control of a β-estradiol-inducible GEV promoter system. Furthermore, additional coexpression of an ER chaperone (e.g., Pdi1p or Emc1p) is essential to boost the PM transport efficiency, allowing the analysis of trafficking-related research questions. Especially for genome-wide screening approaches, a genomic integration of kAE1 should be considered to reduce plasmid-mediated kAE1 expression fluctuations. In such an optimized yeast system, one could not only analyse trafficking of wild-type kAE1 in more detail but also investigate the effect of various dominant and recessive dRTA-causing mutations or truncations on kAE1 transport and UPR activation. To our knowledge, in mammalian cells, relatively little is known if kAE1 mutations trigger UPR and/or ERAD-mediated degradation and whether this degradation is associated with dRTA development.

Collectively, our study highlighted the manifold options of yeast as model system to investigate specific aspects of kAE1 physiology in the future. Moreover, our data provide—for the first time—deeper insight in the intracellular transport of human kAE1 in *S. cerevisiae* and illustrate the reason and consequences of its tremendous accumulation seen in the recent EM study. Finally, we further provide a simple strategy to prevent the intracellular trapping of the human anion exchanger, enabling an improved kAE1 targeting to the yeast cell surface. With this novel knowledge, we believe that genome-wide screenings to identify candidate genes involved in kAE1 transport are now imaginable and will hopefully initiate further kAE1-related research in *S. cerevisiae*.

# 4 | MATERIALS AND METHODS

## 4.1 | Cultivation and transformation of yeast cells

Yeast cultivation was routinely performed at 30°C and 220 rpm in shaking flasks using standard YPD, synthetic complete or drop/out media containing 2% glucose or 3% galactose. *S. cerevisiae* strains used in this study are listed in Table S1. A previously described standard protocol was used for yeast transformation (Becker et al., 2016).

## 4.2 | Vector construction

For construction of the different kAE1 expression plasmids pYES-kAE1$^{FLAG}$, pYES-kAE1$^{1-491}$ and pYES-kAE1$^{1-666}$, a synthetic cDNA of a corresponding yeast codon-optimized kAE1 sequence (GeneArts, ThermoScientific; Appendix S1A–C) was integrated into pYES2.1 (ThermoScientific) via TOPO cloning and correct integration was subsequently checked via *Xba*I/*Bam*H digestion. Construction of the expression plasmids pYES-kAE1$^{WT}$, pYES-kAE1$^{HA}$, pYES-kAE1$^{B3mem}$ and pYES-yeGFP-kAE1 has already been described previously (Sarder et al., 2020). By following manufacturer's instructions, pYES-kAE1$^{E681Q}$ was generated by site-directed mutagenesis using a Q5 mutagenesis kit (Neb), specific primers (Table S2) and pYES-kAE1$^{WT}$ as template. Wild-type Erd2p C-terminally extended by a V5-epitope tag was constructed by conventional PCR using primers listed in Table S2 and finally integrated into pYES2.1 via TOPO cloning to obtain pYES-ERD2$^{V5}$.

## 4.3 | Chromosomal integration of Pma1p-mRFP in Δ*ist2* cells via homologous recombination

For chromosomal integration of the mRFP-tagged PM marker Pma1p, plasmid YIp128-Pma1-mRFP (Grossmann et al., 2007) was initially linearized with *Bgl*II, separated via agarose gel electrophoresis and subsequently purified via a gel extraction kit (Omega). Then, Δ*ist2* BY4741 cells (Papouskova et al., 2017) were transformed with the linearized plasmid and selected on leucine d/o plates at 30°C for at least 3 days. Successful homologous recombination of selected clones was verified by Western blot analysis (data not shown) and SIM.

## 4.4 | Monitoring of UPR activation via Kar2p expression

In brief, cells carrying the indicated plasmids were inoculated in 5 ml of the appropriated d/o glucose medium for 18 h. For inducing *GAL1* promoter-driven protein expression, cells (300–500 μl) were shifted to 10 ml of the appropriate d/o galactose medium and grown to OD$_{600}$ = 0.6–0.8. For ER stress induction, cells carrying an EV were additionally treated with 2.5 mM DTT or 2 μg/ml TM for 6 h. Next, cell pellets (OD$_{600}$ = 5) were harvested at 8000 rpm for 5 min,

washed twice with distilled H$_2$O and resuspended in 200-μl homogenization buffer (10 mM Tris, 1 mM EDTA, 1 mM PMSF, 0.1% β-mercaptoethanol, pH 7.4) containing protease inhibitors (EDTA-free, Roche). For cell lysis, samples were disrupted by a beat beater (Precellys Evolution, Peqlab) using glass beads and the following parameters: 6000 rpm, 3 × 20-s shaking interval, 30-s break/interval. After incubation of the cell lysates at 37°C for 15 min, cell debris were removed by a single centrifugation step at 4°C and 14,000 rpm (10 min), and supernatants were directly used for SDS-PAGE and immunoblotting.

## 4.5 | Growth assay

Precultures of wild-type BY4742 cells containing EV or different kAE1 expression plasmids (pYES-kAE1$^{HA}$, pYES-kAE1$^{WT}$, pYES-kAE1$^{B3mem}$ or pYES-kAE1$^{E681Q}$) were grown overnight at 30°C and 220 rpm in uracil d/o glucose medium. For protein expression, cells were diluted to starting OD$_{600}$ = 0.1 in 50-ml uracil d/o galactose medium, and OD$_{600}$ was measured every 90 min over 30 h. For yeast growth rate calculation, measured OD$_{600}$ values of the different independent biological triplicates were plotted as a function of time, and data were fitted by exponential regression. Based on the obtained equation, mean growth rates per hour (curve slope) ± SD were determined.

## 4.6 | UPR-dependent *lacZ* reporter assay

Fresh overnight precultures of cells carrying EV (pYES) or different kAE1 expression plasmids (pYES-kAE1$^{HA}$, pYES-kAE1$^{FLAG}$ or pYES-kAE1$^{WT}$) were grown in 5-ml uracil d/o glucose medium and cultivated for 18 h at 30°C and 220 rpm. For inducing protein expression, 5-ml uracil d/o galactose medium was inoculated with 300–500 μl of the preculture, and cells were grown to OD$_{600}$ = 0.6–0.8 at 30°C and 220 rpm. Cell harvesting and disruption was identically performed as described above (see monitoring of UPR activation via Kar2p expression). Finally, cell debris were removed by centrifugation at 4°C and 14,000 rpm for 10 min, and 200-μl supernatant was mixed with 100-μl PBS buffer (pH 7.4) containing 500-μg/ml X-gal (Applichem, Darmstadt, Germany). After incubation at 30°C for 24 h, β-galactosidase activity was photographically recorded, and the generation of the blue end product 5,5′-dibromo-4,4′-dichloro-indigo was measured with a spectraphotometer at 615 nm.

## 4.7 | Hac1 splicing reporter-based UPR detection assay

BY4741-SR-GFP cells (Lajoie et al., 2012) were initially transformed with the EV (pYES) or the indicated kAE1 expression plasmid (pYES-kAE1$^{HA}$, pYES-kAE1$^{FLAG}$, pYES-kAE1$^{WT}$ and pYES-kAE1$^{E681Q}$). For inducing kAE1 expression, the different strains were initially

cultivated in 5-ml uracil d/o glucose medium and subsequently shifted to 5-ml uracil d/o galactose medium for 18 h at 30°C and 220 rpm. To induce ER stress, cells carrying an EV were additionally treated with 2.5 mM DTT or 2-µg/ml TM for 6 h. Finally, 10-µl aliquots were spotted on poly-L-lysine-coated cover slips and incubated for 15 min to prevent cell movement during microscopy. To visualize UPR activation, GFP expression levels were monitored via Western blot or fluorescence microscopy using a Keyence BZ-8000 microscope (100x Oil immersion Plan Apo VC objective [1.4 NA]) with the preinstalled filter sets and standard settings for GFP (488 nm).

## 4.8 | EM analysis

Sample preparation, immunostaining and image acquisition were performed as previously described (Sarder et al., 2020). In brief, log phase yeast cultures ($OD_{600} = 0.6$–0.8) of $\Delta end3$ cells expressing full-length kAE1 or EV were filtered into a paste which was pipetted into 0.2-mm-deep aluminium carrier (Engineering Office M. Wohlwend GmbH, Sennwald, Switzerland) and cryo-immobilized by high-pressure freezing using hpm010 (ABRA fluid, Widnau, Switzerland). After different freeze substitution steps (EM-AFS2, Leica Microsystems, Vienna, Austria), samples were exposed to UV to polymerize the Lowicryl matrix. Next, thin sections (70 nm) were cut with a Leica UC6 microtome (Leica Microsystems, Vienna, Austria) and collected on Formvar-coated copper slot grids. Immunogold labelling was done by floating grids on drops of blocking buffer consisting of 1.5% BSA and 0.1% fish skin gelatine in PBS for 30 min, followed by incubation with anti-kAE1 antibodies (BRIC170, IBGRL, Bristol, UK) diluted 1:100 in blocking buffer for 30 min. Samples were then incubated with anti-mouse antibody (Dako, #Z025902-2) and subsequently 10-nm gold-conjugated protein A (CMC University Medical Center, Utrecht, Netherlands) for 20 min. Between each incubation step, grids were washed with five drops of PBS. After fixation in glutaraldehyde and post staining using uranyl acetate and lead citrate, sections were analysed using a JEOL JEM-1400 electron microscope (JEOL, Tokyo) operating at 80 kV and equipped with a 4K TemCam F416 (Tietz Video and Image Processing Systems GmBH, Gautig). Image analysis and processing was conducted with Fiji software (Schindelin et al., 2012).

## 4.9 | Structured illumination microscopy

In brief, cells were spotted on 25-mm round glass cover slips (Warner Instruments) following an 1-h incubation period to let them settle down to prevent cell movement during the experiment. Next, SIM images were acquired using an inverted Elyra PS1 microscopic system (Carl Zeiss Microscopy, GmbH, Jena) equipped with a 63× Plan-Apochromat objective (NA = 1.4, Carl Zeiss Microscopy, GmbH, Jena). Samples were illuminated with the corresponding excitation wavelength for GFP, mRFP and mCherry. Acquisition and super resolution processing were performed with Zen 2012 software (Carl Zeiss,

Microscopy GmbH, Jena, Germany). Further image analysis was carried out with the Fiji software (Schindelin et al., 2012). For observing dim structures, brightness and contrast of each fluorescence channel were separately adjusted.

## 4.10 | SDS-PAGE and Western blot analysis

SDS-PAGE was performed under nonreducing conditions in 10% Tris-Tricine gels using a buffer system as previously described (Ploug et al., 1989). By performing semidry blotting (Jacobson & Kårsnäs, 1990), proteins were subsequently transferred onto PVDF membranes in the presence of transfer buffer (25 mM Tris, 190 mM glycine, 0.1% SDS, 20% methanol). Usually, kAE1 expression was validated using primary anti-kAE1 antibodies (BRIC170, recognizing an epitope in the amino acid region of 368–382) and visualized with secondary HRP-conjugated anti-rabbit antibodies. For Kar2p detection, blots were probed with anti-Kar2p and anti-rabbit-HRP antibodies. To monitor expression of yeGFP-kAE1, blots were probed with anti-GFP and anti-mouse-HRP antibodies. For visualization of the loading control Pgk1p (phosphoglycerate kinase 1), Western blots were incubated with anti-Pgk1 and HRP-coupled anti-rabbit antibodies. Finally, PVDF membranes were incubated with SuperSignalTM West Femto Maximum Sensitivity Substrate (ThermoScientific), and protein signals were visualized with Amersham Imager 600 (GE Healthcare). All antibody dilutions and sources are listed in Table S3.

## 4.11 | β-Estradiol assay

Construction of BY4742 GEV strain is already described in (Sarder et al., 2020). For stepwise induction of kAE1 expression, 300 µl of a fresh overnight culture of BY4742 GEV cells expressing an EV (BY4742 GEV [pYES-EV]) or HA-tagged kAE1 (BY4242 GEV [pYES-kAE1$^{HA}$]) was cultivated in 5-ml uracil d/o glucose containing different concentrations of β-estradiol (0, 1, 10, $10^2$, $10^3$, $5 \times 10^3$ and $10^4$ nM) for 18 h at 30°C and 220 rpm. Then, cells ($OD_{600} = 10$) were harvested for 5 min at 8000 rpm, subsequently washed twice with distilled $H_2O$ and lysed in 200-µl SDS sample buffer supplemented with a protease inhibitor cocktail (Roche) by using a beat beater (Precellys Evolution, Peqlab). After 15-min incubation at 37°C and an additional centrifugation step (15 min, 13,000 rpm, 4°C), supernatants were subjected to SDS-PAGE and immunoblotting.

## 4.12 | Data analysis and statistics

Statistical analysis was carried out in GraphPad Prism 8 (GraphPad Software, San Diego, California, USA). All pooled data were given as mean values ± SEM (unless otherwise stated). Statistical significance was assessed by one-way ANOVA based on biological replicates and at sample sizes of $n \geq 3$ independent experiments (ns, not significant; *$p < 0.05$; **$p < 0.01$; ***$p < 0.001$).

## CONFLICT OF INTEREST

No conflict of interest declared.

## AUTHOR CONTRIBUTIONS

BB, EC and MJS designed the whole study. XL performed all experiments, conducted data analysis and wrote parts of the manuscript. BB and MJS wrote the majority of the manuscript and designed the study.

## ORCID

*Björn Becker* https://orcid.org/0000-0003-0057-8622

## REFERENCES

Almomani, E. Y., King, J. C., Netsawang, J., Yenchitsomanus, P. T., Malasit, P., Limjindaporn, T., Alexander, R. T., & Cordat, E. (2012). Adaptor protein 1 complexes regulate intracellular trafficking of the kidney anion exchanger 1 in epithelial cells. *American Journal of Physiology-Cell Physiology*, *303*(5), C554–C566. https://doi.org/10.1152/ajpcell.00124.2012

Alper, S. L. (2010). Familial renal tubular acidosis. *Journal of Nephrology*, *23*, S57–S76.PMID: 21170890

Alper, S. L., Darman, R. B., Chernova, M. N., & Dahl, N. K. (2002). The AE gene family of Cl/HCO$_3^-$ exchangers. *Journal of Nephrology*, *15*, S41–S53. PMID: 12027221.

Becker, B., Blum, A., Gießelmann, E., Dausend, J., Rammo, D., Müller, N. C., Tschacksch, E., Steimer, M., Spindler, J., Becherer, U., & Rettig, J. (2016). H/KDEL receptors mediate host cell intoxication by a viral A/B toxin in yeast. *Scientific Reports*, *6*(1), 1–11. https://doi.org/10.1038/srep31105

Beckmann, R., Toye, A. M., Smythe, J. S., Anstee, D. J., & Tanner, M. J. (2002). An N-terminal GFP tag does not alter the functional expression to the plasma membrane of red cell and kidney anion exchanger (AE1) in mammalian cells. *Molecular Membrane Biology*, *19*(3), 187–200. https://doi.org/10.1080/09687680210141043

Berner, N., Reutter, K. R., & Wolf, D. H. (2018). Protein quality control of the endoplasmic reticulum and ubiquitin–proteasome-triggered degradation of aberrant proteins: Yeast pioneers the path. *Annual Review of Biochemistry*, *87*, 751–782. https://doi.org/10.1146/annurev-biochem-062917-012749

Bonar, P., & Casey, J. R. (2010). Purification of functional human Cl$^-$/HCO$_3^-$ exchanger, AE1, over-expressed in *Saccharomyces cerevisiae*. *Protein Expression and Purification*, *74*(1), 106–115. https://doi.org/10.1016/j.pep.2010.06.020

Chang, H. J., Jesch, S. A., Gaspar, M. L., & Henry, S. A. (2004). Role of the unfolded protein response pathway in secretory stress and regulation of INO1 expression in *Saccharomyces cerevisiae*. *Genetics*, *168*(4), 1899–1913. https://doi.org/10.1534/genetics.104.032961

Chen, W., Feng, Y., Chen, D., & Wandinger-Ness, A. (1998). Rab11 is required for trans-Golgi network–to–plasma membrane transport and a preferential target for GDP dissociation inhibitor. *Molecular Biology of the Cell*, *9*, 3241–3211, 3257. https://doi.org/10.1091/mbc.9.11.3241

Cordat, E., & Casey, J. R. (2009). Bicarbonate transport in cell physiology and disease. *Biochemical Journal*, *417*(2), 423–439. https://doi.org/10.1042/bj20081634

Cordat, E., Kittanakom, S., Yenchitsomanus, P. T., Li, J., Du, K., Lukacs, G. L., & Reithmeier, R. A. (2006). Dominant and recessive distal renal tubular acidosis mutations of kidney anion exchanger 1 induce distinct trafficking defects in MDCK cells. *Traffic*, *7*(2), 117–128. https://doi.org/10.1111/j.1600-0854.2005.00366.x

Coudray, N., Seyler, S. L., Lasala, R., Zhang, Z., Clark, K. M., Dumont, M. E., Rohou, A., Beckstein, O., & Stokes, D. L. (2017). Structure of the SLC4 transporter Bor1p in an inward-facing conformation. *Protein Science*, *26*(1), 130–145. https://doi.org/10.1002/pro.3061

Devonald, M. A., Smith, A. N., Poon, J. P., Ihrke, G., & Karet, F. E. (2003). Non-polarized targeting of AE1 causes autosomal dominant distal renal tubular acidosis. *Nature Genetics*, *33*(2), 125–127. https://doi.org/10.1038/ng1082

Gardner, B. M., & Walter, P. (2011). Unfolded proteins are Ire1-activating ligands that directly induce the unfolded protein response. *Science*, *333*(6051), 1891–1894. https://doi.org/10.1126/science.1209126

Grossmann, G., Opekarova, M., Malinsky, J., Weig-Meckl, I., & Tanner, W. (2007). Membrane potential governs lateral segregation of plasma membrane proteins and lipids in yeast. *The EMBO Journal*, *26*(1), 1–8. https://doi.org/10.1240/sav_gbm_2007_m_001710

Groves, J. D., Falson, P., Le Maire, M., & Tanner, M. J. (1996). Functional cell surface expression of the anion transport domain of human red cell band 3 (AE1) in the yeast *Saccharomyces cerevisiae*. *Proceedings of the National Academy of Sciences*, *93*(22), 12245–12250. https://doi.org/10.1073/pnas.93.22.12245

Groves, J. D., Parker, M. D., Askin, D., Falson, P., le Maire, M., & Tanner, M. J. (1999). Heterologous expression of the red-cell anion exchanger (band 3; AEI). *Biochemical Society Transactions*, *27*(6), 917–923. https://doi.org/10.1042/bst0270917

Groves, J. D., & Tanner, M. J. (1992). Glycophorin A facilitates the expression of human band 3-mediated anion transport in Xenopus oocytes. *Journal of Biological Chemistry*, *267*(31), 22163–22170. https://doi.org/10.1016/s0021-9258(18)41649-3

Groves, J. D., & Tanner, M. J. (1994). Role of N-glycosylation in the expression of human band 3-mediated anion transport. *Molecular Membrane Biology*, *11*(1), 31–38. https://doi.org/10.1007/bf00234488

Hou, J., Tyo, K. E., Liu, Z., Petranovic, D., & Nielsen, J. (2012). Metabolic engineering of recombinant protein secretion by *Saccharomyces cerevisiae*. *FEMS Yeast Research*, *12*(5), 491–510. https://doi.org/10.1111/j.1567-1364.2012.00810.x

Jacobson, G., & Kårsnäs, P. (1990). Important parameters in semi-dry electrophoretic transfer. *Electrophoresis*, *11*(1), 46–52. https://doi.org/10.1002/elps.1150110111

Jennings, M. L., & Smith, J. S. (1992). Anion-proton cotransport through the human red blood cell band 3 protein. Role of glutamate 681. *Journal of Biological Chemistry*, *267*(20), 13964–13971. https://doi.org/10.1016/s0021-9258(19)49664-6

Junking, M., Sawasdee, N., Duangtum, N., Cheunsuchon, B., Limjindaporn, T., & Yenchitsomanus, P. T. (2014). Role of adaptor proteins and clathrin in the trafficking of human kidney anion exchanger 1 (kAE1) to the cell surface. *Traffic*, *15*(7), 788–802. https://doi.org/10.1111/tra.12172

Kimata, Y., & Kohno, K. (2011). Endoplasmic reticulum stress-sensing mechanisms in yeast and mammalian cells. *Current Opinion in Cell Biology*, *23*(2), 135–142. https://doi.org/10.1016/j.ceb.2010.10.008

Kintaka, R., Makanae, K., & Moriya, H. (2016). Cellular growth defects triggered by an overload of protein localization processes. *Scientific Reports*, 6(1), 1–11. https://doi.org/10.1038/srep31774

Kolb, A. R., Buck, T. M., & Brodsky, J. L. (2011). *Saccharomyces cerivisiae* as a model system for kidney disease: What can yeast tell us about renal function? *American Journal of Physiology-Renal Physiology*, 301(1), F1–F11. https://doi.org/10.1152/ajprenal.00141.2011

Lajoie, P., Moir, R. D., Willis, I. M., & Snapp, E. L. (2012). Kar2p availability defines distinct forms of endoplasmic reticulum stress in living cells. *Molecular Biology of the Cell*, 23(5), 955–964. https://doi.org/10.1091/mbc.e11-12-0995

Lamppa, J. W., Tanyos, S. A., & Griswold, K. E. (2013). Engineering *Escherichia coli* for soluble expression and single step purification of active human lysozyme. *Journal of Biotechnology*, 164(1), 1–8. https://doi.org/10.1016/j.jbiotec.2012.11.007

Lashhab, R., Rumley, A. C., Arutyunov, D., Rizvi, M., You, C., Dimke, H., Touret, N., Zimmermann, R., Jung, M., Chen, X. Z., & Alexander, T. (2019). The kidney anion exchanger 1 affects tight junction properties via claudin-4. *Scientific Reports*, 9(1), 1–16. https://doi.org/10.1038/s41598-019-39430-9

Lashhab, R., Ullah, A. S., & Cordat, E. (2018). Renal collecting duct physiology and pathophysiology. *Biochemistry and Cell Biology*, 97(3), 234–242. https://doi.org/10.1139/bcb-2018-0192

Mackie, T. D., & Brodsky, J. L. (2018). Investigating potassium channels in budding yeast: A genetic sandbox. *Genetics*, 209(3), 637–650. https://doi.org/10.1534/genetics.118.301026

Manford, A. G., Stefan, C. J., Yuan, H. L., MacGurn, J. A., & Emr, S. D. (2012). ER-to-plasma membrane tethering proteins regulate cell signaling and ER morphology. *Developmental Cell*, 23(6), 1129–1140. https://doi.org/10.1016/j.devcel.2012.11.004

McIsaac, R. S., Silverman, S. J., McClean, M. N., Gibney, P. A., Macinskas, J., Hickman, M. J., Petti, A. A., & Botstein, D. (2011). Fast-acting and nearly gratuitous induction of gene expression and protein depletion in *Saccharomyces cerevisiae*. *Molecular Biology of the Cell*, 22(22), 4447–4459. https://doi.org/10.1091/mbc.e11-05-0466

Nishihara, K., Kanemori, M., Kitagawa, M., Yanagi, H., & Yura, T. (1998). Chaperone coexpression plasmids: Differential and synergistic roles of DnaK-DnaJ-GrpE and GroEL-GroES in assisting folding of an allergen of Japanese cedar pollen, Cryj2, in *Escherichia coli*. *Applied and Environmental Microbiology*, 64(5), 1694–1699. https://doi.org/10.1128/aem.64.5.1694-1699.1998

Papouskova, K., Andrsova, M., & Sychrova, H. (2017). Lack of cortical endoplasmic reticulum protein Ist2 alters sodium accumulation in *Saccharomyces cerevisiae* cells. *FEMS Yeast Research*, 17(2), fox011. https://doi.org/10.1093/femsyr/fox011

Parmar, H. B., & Duncan, R. (2016). A novel tribasic Golgi export signal directs cargo protein interaction with activated Rab11 and AP-1–dependent Golgi–plasma membrane trafficking. *Molecular Biology of the Cell*, 27(8), 1320–1331. https://doi.org/10.1091/mbc.e15-12-0845

Ploug, M., Jensen, A. L., & Barkholt, V. (1989). Determination of amino acid compositions and NH2-terminal sequences of peptides electroblotted onto PVDF membranes from tricine-sodium dodecyl sulfate-polyacrylamide gel electrophoresis: Application to peptide mapping of human complement component C3. *Analytical Biochemistry*, 181(1), 33–39. https://doi.org/10.1016/0003-2697(89)90390-4

Reithmeier, R. A., Casey, J. R., Kalli, A. C., Sansom, M. S., Alguel, Y., & Iwata, S. (2016). Band 3, the human red cell chloride/bicarbonate anion exchanger (AE1, SLC4A1), in a structural context. *Biochimica et Biophysica Acta (BBA)-Biomembranes*, 1858(7), 1507–1532. https://doi.org/10.1016/j.bbamem.2016.03.030

Romanos, M. A., Scorer, C. A., & Clare, J. J. (1992). Foreign gene expression in yeast: A review. *Yeast*, 8(6), 423–488. https://doi.org/10.1002/yea.320080602

Roy, A., Al-bataineh, M. M., & Pastor-Soler, N. M. (2015). Collecting duct intercalated cell function and regulation. *Clinical Journal of the American Society of Nephrology*, 10(2), 305–324. https://doi.org/10.3410/f.725330507.793505796

Sarder, H. A., Li, X., Funaya, C., Cordat, E., Schmitt, M. J., & Becker, B. (2020). *Saccharomyces cerevisiae*: First steps to a suitable model system to study the function and intracellular transport of human kidney anion exchanger 1. *mSphere*, 5(1). https://doi.org/10.1128/msphere.00802-19

Schindelin, J., Arganda-Carreras, I., Frise, E., Kaynig, V., Longair, M., Pietzsch, T., Preibisch, S., Rueden, C., Saalfeld, S., Schmid, B., & Tinevez, J. Y. (2012). Fiji: An open-source platform for biological-image analysis. *Nature Methods*, 9(7), 676–682. https://doi.org/10.1038/nmeth.2019

Semenza, J. C., Hardwick, K. G., Dean, N., & Pelham, H. R. (1990). ERD2, a yeast gene required for the receptor-mediated retrieval of luminal ER proteins from the secretory pathway. *Cell*, 61(7), 1349–1357. https://doi.org/10.1016/0092-8674(90)90698-e

Shurtleff, M. J., Itzhak, D. N., Hussmann, J. A., Oakdale, N. T. S., Costa, E. A., Jonikas, M., Weibezahn, J., Popova, K. D., Jan, C. H., Sinitcyn, P., & Vembar, S. S. (2018). The ER membrane protein complex interacts cotranslationally to enable biogenesis of multipass membrane proteins. *eLife*, 7, e37018. https://doi.org/10.7554/elife.37018.023

Sidrauski, C., & Walter, P. (1997). The transmembrane kinase Ire1p is a site-specific endonuclease that initiates mRNA splicing in the unfolded protein response. *Cell*, 90(6), 1031–1039. https://doi.org/10.1016/s0092-8674(00)80369-4

Spang, A. (2015). The road not taken: less traveled roads from the TGN to the plasma membrane. *Membranes*, 5(1), 84–98. https://doi.org/10.3390/membranes5010084

Su, Y., Blake-Palmer, K. G., Fry, A. C., Best, A., Brown, A. C., Hiemstra, T. F., Horita, S., Zhou, A., Toye, A. M., & Karet, F. E. (2011). Glyceraldehyde 3-phosphate dehydrogenase is required for band 3 (anion exchanger 1) membrane residency in the mammalian kidney. *American Journal of Physiology-Renal Physiology*, 300(1), F157–F166. https://doi.org/10.1152/ajprenal.00228.2010

Su, Y., Hiemstra, T. F., Yan, Y., Li, J., Karet, H. I., Rosen, L., Moreno, P., & Frankl, F. E. K. (2017). PDLIM5 links kidney anion exchanger 1 (kAE1) to ILK and is required for membrane targeting of kAE1. *Scientific Reports*, 7(1), 39701. https://doi.org/10.1038/srep39701

Thurtle-Schmidt, B. H., & Stroud, R. M. (2016). Structure of Bor1 supports an elevator transport mechanism for SLC4 anion exchangers. *Proceedings of the National Academy of Sciences*, 113(38), 10542–10546. https://doi.org/10.1073/pnas.1612603113

Toye, A. M., Banting, G., & Tanner, M. J. (2004). Regions of human kidney anion exchanger 1 (kAE1) required for basolateral targeting of kAE1 in polarised kidney cells: Mis-targeting explains dominant renal tubular acidosis (dRTA). *Journal of Cell Science*, 117(8), 1399–1410. https://doi.org/10.1242/jcs.00974

Trepiccione, F., Prosperi, F., de la Motte, L. R., Hübner, C. A., Chambrey, R., Eladari, D., & Capasso, G. (2017). New findings on the pathogenesis of distal renal tubular acidosis. *Kidney Diseases*, 3(3), 98–105. https://doi.org/10.1159/000478781

Umebayashi, K., Hirata, A., Fukuda, R., Horiuchi, H., Ohta, A., & Takagi, M. (1997). Accumulation of misfolded protein aggregates leads to the formation of Russell body-like dilated endoplasmic reticulum in yeast. *Yeast*, 13(11), 1009–1020. https://doi.org/10.1002/(sici)1097-0061(19970915)13:11%3C1009::aid-yea157%3E3.0.co;2-k

Wakana, Y., Van Galen, J., Meissner, F., Scarpa, M., Polishchuk, R. S., Mann, M., & Malhotra, V. (2012). A new class of carriers that transport selective cargo from the trans Golgi network to the cell surface. *The EMBO Journal*, 31(20), 3976–3990. https://doi.org/10.1038/emboj.2012.235

Wang, C. W., Hamamoto, S., Orci, L., & Schekman, R. (2006). Exomer: A coat complex for transport of select membrane proteins from the

trans-Golgi network to the plasma membrane in yeast. *The Journal of Cell Biology*, *174*(7), 973–983. https://doi.org/10.1083/jcb.200605106

Weill, U., Arakel, E. C., Goldmann, O., Golan, M., Chuartzman, S., Munro, S., Schwappach, B., & Schuldiner, M. (2018). Toolbox: Creating a systematic database of secretory pathway proteins uncovers new cargo for COPI. *Traffic*, *19*(5), 370–379. https://doi.org/10.1111/tra.12560

Weill, U., Yofe, I., Sass, E., Stynen, B., Davidi, D., Natarajan, J., Ben-Menachem, R., Avihou, Z., Goldman, O., Harpaz, N., & Chuartzman, S. (2018). Genome-wide SWAp-Tag yeast libraries for proteome exploration. *Nature Methods*, *15*(8), 617–622. https://doi.org/10.1038/s41592-018-0044-9

Welihinda, A. A., Tirasophon, W., & Kaufman, R. J. (1999). The cellular response to protein misfolding in the endoplasmic reticulum. *Gene Expression: The Journal of Liver Research*, *7*(4–5), 293–300. PMID: 10440230.

Winters, C. M., & Chiang, H. L. (2016). Yeast as a model system to study trafficking of small vesicles carrying signal-less proteins in and out of the cell. *Current Protein and Peptide Science*, *17*(8), 808–820. https://doi.org/10.2174/1389203717666160226144457

Wolf, W., Kilic, A., Schrul, B., Lorenz, H., Schwappach, B., & Seedorf, M. (2012). Yeast Ist2 recruits the endoplasmic reticulum to the plasma membrane and creates a ribosome-free membrane microcompartment. *PLoS ONE*, *7*(7), e39703. https://doi.org/10.1371/journal.pone.0039703

Young, M. T., Beckmann, R., Toye, A. M., & Tanner, M. J. (2000). Red-cell glycophorin A–band 3 interactions associated with the movement of band 3 to the cell surface. *Biochemical Journal*, *350*(1), 53–60. https://doi.org/10.1042/0264-6021:3500053

## SUPPORTING INFORMATION

Additional supporting information may be found online in the Supporting Information section at the end of this article.